Angewandte Chemie
Eine Zeitschrift der Gesellschaft Deutscher Chemiker

Supporting Information

Optogenetic Control of Voltage-Gated Calcium Channels

Guolin Ma[+], Jindou Liu[+], Yuepeng Ke[+], Xin Liu, Minyong Li, Fen Wang, Gang Han, Yun Huang, Youjun Wang, and Yubin Zhou**

anie_201713080_sm_miscellaneous_information.pdf
anie_201713080_sm_Movie_S1.avi
anie_201713080_sm_Movie_S2.avi
anie_201713080_sm_Movie_S3.avi
anie_201713080_sm_Movie_S4.avi
anie_201713080_sm_Movie_S5.avi

Supporting Information

Contents:

Materials and Methods

Chemicals and reagents

The calcium indicator Fluo-4 AM (Cat No. F14201) was purchased form Life Technologies (Carlsbad, CA, USA). Cal-590^{TM} AM (Cat N. 20510) was purchased from AAT Bioquest, Inc. Claycomb Medium, Norepinephrine, L-glutamine, potassium chloride (KCl) and other reagents were purchased from Sigma-Aldrich unless otherwise indicated.

Design and construction of engineered Rem plasmids

cDNA encoding the human Rem was purchased from DNASU (ID: HsCD00632798) and served as a template for amplifying Rem fragments. To produce chimeric combinations of Rem and sspB with varying lengths of linkers, the fragments of human Rem and sspB with linkers were prepared by standard PCR using a KOD hot start DNA polymerase (EMD Millipore, Billerica, MA, USA) and then inserted into mCherry (mCh) tagged pcDNA 3.1 (+) vector (Invitrogen) using the NEBuilder HiFi DNA assembly kits (New England BioLabs). mCh-L1-Rem$_{1\text{-}266}$-L2-sspB and mCh-L1-sspB-L2-Rem$_{1\text{-}266}$ (L1 and L2 as linkers were summarized in Figure S1) were generated using this method. To make YFP or CFP tagged Rem$_{1\text{-}266}$-sspB, Rem$_{1\text{-}266}$-sspB with an appropriate linker was amplified from mCherry-L1-Rem1$_{1\text{-}266}$-L2-sspB and inserted into the pEYFP-N1 or pECFP-N1 vector (Clontech) using XhoI and BamHI restriction sites. Venus-iLID-CAAX (CAAX motif from KRas4B) was a gift from Brian Kuhlman (Addgene # 60411). Lyn11-iLiD-GFP was prepared by amplifying iLID from Venus-iLID-CAAX and then sub-cloned into the pcDNA 3.1 (+) vector between the BamHI and EcoRI sites. Then Lyn11 and GFP were separately inserted into pcDNA 3.1 (+)-iLID by using restriction sites of NheI/BamHI (for Lyn11) and EcoRI/XhoI (for GFP). To generate a multicistronic vector with coexpression of Rem$_{1\text{-}266}$-sspB and iLID-CAAX, a self-cleaving 2A peptide (P2A) was employed[1]. mCherry-L1-Rem$_{1\text{-}266}$-L2-ssPB, P2A peptide and iLID-CAAX were amplified separately and then assembled into the pTriEx 1.1 vector (Novagen, EMD Millipore) by using the HiFi DNA assembly kits, thus producing mCh-L1-Rem$_{1\text{-}266}$-L2-ssPB-P2A-iLID-CAAX (OptoRGK, L1 = GSGGS, L2 = EFGSGGGSGS). CFP tagged optoRGK was achieved to replace mCh tag by CFP tag using standard PCR method and HiFi DNA assembly kits. The genetically encoded calcium sensors, pGP-CMV-GCaMP6m (#40754) and pGP-CMV-NES-jRCaMP1b (#63136), were obtained from Addgene.

Cell culture and transfection

HeLa, human embryonic kidney (HEK293T), and mouse myoblast C2C12 cell lines were obtained from the American Type Culture Collection (ATCC) and cultured in Dulbecco's modified Eagle's medium (DMEM, Sigma-Aldrich), supplemented with 10% heat-inactivated fetal bovine serum, 100 U/ml penicillin/ streptomycin at 37 °C with 5% CO2. HEK293 cells stably expressing the human $Ca_V1.2$ L-type Ca channel (designated HEK-$Ca_V1.2$) is derived from a C1-6-37-3 parent line[2]. HL-1 cardiac muscle cell line was purchased from Sigma-Aldrich and cultured in Claycomb Medium (Sigma-Aldrich) with 100 µM norepinephrine, 10% Fetal Bovine Serum (FBS) and 2 mM L-glutamine[3]. The culture flasks and glass bottom dishes for fluorescence microscopy were coated with gelatin/fibronectin before culturing HL-1 cells.

Transfection was performed by using Lipofectamine 3000 (Life Technologies) following the manufacturer's recommended protocol. Lipofectamine transfection reagents typically resulted in approximately 80% and 40 % transfection efficiency in HeLa/HEK293T and C2C12 cells[4], respectively. Transfection of HL-1 cells using Lipofectamine was performed as previously described[5]. 2 µg of DNA in 50 µL of Opti-Mem and was mixed well with 3 µL of Lipofectamine 3000 reagents in 50 µL of Opti-MEM. After incubation 20 min, the mixture was dropped in to HL-1 cells with norepinephrine-free and penicillin/streptomycin-free Claycomb Medium (with 5%

serum). Cells were incubated in a humidified tissue culture incubator at 37 °C in 95% air, 5% CO2 for 12 h. Then, transfection medium was replaced with normal supplemented Claycomb Medium. The transfection efficiency in HL-1 cells was ~30% [5b, 5c, 6].

Confocal imaging for protein translocation

To monitor the light-inducible shuttling of engineered Rem/sspB chimeras between the cytosol and the plasma membrane (PM), 100 ~ 200 ng plasmids were transfected into HeLa or other indicated cells. 24 ~ 48 hours after transfection, imaging experiments were carried out at room temperature with 40× oil lens on an inverted Nikon Eclipse Ti-E microscope by using argon-ion (405 nm and 488 nm) and helium-neon (543 nm) or diode (561 nm) as laser sources. Photostimulation was achieved by using an external blue LED (470 nm, 40 $\mu W/mm^2$, ThorLabs Inc., Newton, NJ, USA) or using the 488-nm laser source from the Nikon A1R+ confocal microscope. Light power density was measured by using an optical power meter from ThorLabs. Light cycles were performed either manually or programmed by Nikon software with 5% 488-nm laser stimulation. Time-lapse imaging of mCherry signal was processed in the dark by turning on only the 561-nm laser channel. Image analysis was performed using the NIS-Elements software (Nikon).

Real-time intracellular Ca^{2+} measurements

For measurements of Ca^{2+} influx in living cells, the red genetically encoded Ca^{2+} indicator jRCaMP1b or Ca^{2+}-sensitive fluorescent dyes (Fluo-4 or Cal-590) were employed. To monitor membrane depolarization triggered Ca^{2+} entry in HEK-Cav1.2 cells, 2 μg of the multicistronic vector CFP tagged optoRGK and 2 μg of cytosolic jRCaMP1b were co-transfected into HEK-Cav1.2 cells. Twenty-four hours after transfection, red Ca^{2+} indicator signals at 562 nm were obtained using a ZEISS oberserver-A1 microscope. The imaging bath solution contains (mM) 107 NaCl, 7.2 KCl, 1.2 $MgCl_2$, 11.5 glucose, 1 Ca^{2+}, 20 HEPES-NaOH (pH 7.2). The Ca^{2+} transients/spikes were elicited with a fast (< 4 sec) bulk flow of equimolar replacement of NaCl with 50 mM KCl. The resulting transients were collected every two seconds. The triggered Ca^{2+} influx quickly fell back to the basal level when switching the extracellular buffer to a low KCl concentration. Because the excitation light for these red Ca^{2+} indicators will not photoactivate the iLID system, both the ON (blue light) and OFF (dark) phases of Ca^{2+} transients triggered by 50 mM KCl can be monitored by applying multiple dark-light cycles with an external pulsed LED light (470 nm at power intensity of 40 $\mu W/mm^2$). After photostimulation, the CFP and Ca^{2+} signals shown by red Ca^{2+} indicators were both captured to separate control cells (no CFP signals) and optoRGK-expressing cells (with CFP signals). The experiments were performed at room temperature. The resulting data collected with MetaFluor software (Molecular Devices) were then exported as txt file, further analyzed with Matlab, and plotted using the Prism 5 software.

For C2C12 myoblasts, Fluo-4 AM was used to monitor cytosolic calcium. 300 ng optoRGK and other engineered Rem constructs were transfected respectively. After 36 h post-transfection, C2C12 cells were loaded with 3 μM Fluo-4 AM in Ca^{2+} free bath buffer (mM, 107 NaCl, 7.2 KCl, 1.2 $MgCl_2$, 11.5 glucose, 20 HEPES-NaOH, pH 7.2) for 30 min at 37°C in a 5% CO_2 humidified incubator. Removal of unincorporated Fluo-4 AM was accomplished by rinsing cells with PBS and then incubating for 20-30 min in imaging bath solution containing (mM) 107 NaCl, 7.2 KCl, 1.2 $MgCl_2$, 11.5 glucose, 1 Ca^{2+}, 20 HEPES-NaOH, pH 7.2. A 488-nm laser on a Nikon Eclipse Ti-E microscope was used to excite Fluo-4 signal, and a 561-nm laser was used to excite mCherry from engineered Rem at intervals of 2 - 4 s. The mCherry-positive cells were selected for statistical analyses. Since the excitation wavelength used to acquire the Fluo-4 signals (488 nm) partially overlaps with the photo-activating wavelengths of iLID (450-500 nm), the interaction between PM-iLID and Rem-sspB was initiated

when the 488-nm laser source was turned on. Therefore, Fluo-4 could only be used to monitor the ON phase of engineered Rem. Data analysis was performed using the NIS-Elements software (Nikon), with the results plotted using the Prism 5 software.

For measurement of Ca^{2+} transients in HL-1 cells, cells were seeded at a density of 3×10^5 cells per 35-mm culture dish with a glass bottom (12 mm diameter), which was pre-treated with gelatin-fibronectin overnight to enhance coating. 300 ng of mCh or CFP tagged optoRGK construct was transfected into HL-1 cells. 36 hours after transfection, HL-1 cells were loaded with 3 µM Fluo-4 AM or Cal-590 with incubation for 30 min at 37 °C with 5% CO_2 in Ca^{2+} free bath solution (mM, 107 NaCl, 7.2 KCl, 1.2 $MgCl_2$, 11.5 glucose, 20 HEPES-NaOH, pH 7.2). Cells were then washed with PBS and incubated at 37°C with 5% CO_2 for 30 min in the supplemented Claycomb media. 488-nm laser or 561-nm laser from Nikon Eclipse Ti-E microscope were used to record Fluo-4 or Cal-590 signals and the data were acquired every 500 msec. Statistical tests on Rem transfected cells in a given field were performed by dividing cells into two groups: cells with visible mCherry (or CFP) signal and cells without visible mCherry (or CFP) signal. Fields were preselected to contain approximately 30% transfected HL-1 cardiac myocytes. The data analysis was mainly performed using the NIS-Elements software (Nikon) and the Rems cellular distribution analysis was analyzed by image J.

Electrophysiological measurements

Whole-cell recordings were performed with an EPC-10 patch-clamp amplifier (HEKA Elektronik) in HEK-$Ca_V1.2$ cells that stably expressing $Ca_V1.2$ channel and other auxiliary subunits at room temperature. 2 µg mCh tagged optoRGK were transfected into HEK-Cav1.2 cells by electroporation. The internal solutions included (in mM): 135 $CsMeSO_3$, 5 $CsCl_2$, 1 MgCl2, 4 MgATP, 5 HEPES, and 5 EGTA, 290 mOsm adjusted with glucose and at pH 7.3 adjusted with CsOH. The bath solution contained (in mM): 140 TEA-$MeSO_3$, 10 HEPES, 10 $BaCl_2$, 300 mOsm adjusted with glucose and at pH 7.3 adjusted with TEAOH. Recording procedures are similar to those reported previously[7]. Data were collected from at least 8 cells for each condition. GFP excitation light (FF02-482/18, Semrock BrightLine) was employed to provide blue light in the dark-light cycles. HEKA Fitmaster and Matlab 2014a software were used for data analysis.

Data analyses

The fluorescence images were analyzed with the NIS-Elements imaging software (Nikon), MetaFluor software (Molecular Devices) and image J. The exported data were plotted by GraphPad Prism 5 graphing and statistical software. The mean lifetime of fluorescence signal change was calculated with a single exponential decay equation F(t) = F(0)*e^(-t/τ). Quantitative data are expressed as the mean and standard error of the mean (s.e.m.) unless otherwise noted. Statistical significance between two groups was determined with a two-tailed Student's *t*-test *P<0.05; **P<0.01; ***P<0.001, when compared to control.

Supplemental References

1. Kim, J. H.; Lee, S. R.; Li, L. H.; Park, H. J.; Park, J. H.; Lee, K. Y.; Kim, M. K.; Shin, B. A.; Choi, S. Y., High cleavage efficiency of a 2A peptide derived from porcine teschovirus-1 in human cell lines, zebrafish and mice. *PloS one* **2011,** *6* (4), e18556.

2. (a) Balasubramanian, B.; Imredy, J. P.; Kim, D.; Penniman, J.; Lagrutta, A.; Salata, J. J., Optimization of Ca(v)1.2 screening with an automated planar patch clamp platform. *Journal of pharmacological and toxicological methods* **2009,** *59* (2), 62-72; (b) Xia, M.; Imredy, J. P.; Koblan, K. S.; Bennett, P.; Connolly, T. M., State-dependent inhibition of L-type calcium channels: cell-based assay in high-throughput format. *Analytical biochemistry* **2004,** *327* (1), 74-81.

3. (a) Claycomb, W. C.; Lanson, N. A., Jr.; Stallworth, B. S.; Egeland, D. B.; Delcarpio, J. B.; Bahinski, A.; Izzo, N. J., Jr., HL-1 cells: a cardiac muscle cell line that contracts and retains phenotypic characteristics of the adult cardiomyocyte. *Proceedings of the National Academy of Sciences of the United States of America* **1998,** *95* (6), 2979-84; (b) Pelloux, S.; Robillard, J.; Ferrera, R.; Bilbaut, A.; Ojeda, C.; Saks, V.; Ovize, M.; Tourneur, Y., Non-beating HL-1 cells for confocal microscopy: application to mitochondrial functions during cardiac preconditioning. *Progress in biophysics and molecular biology* **2006,** *90* (1-3), 270-98.

4. (a) Dodds, E.; Dunckley, M. G.; Naujoks, K.; Michaelis, U.; Dickson, G., Lipofection of cultured mouse muscle cells: a direct comparison of Lipofectamine and DOSPER. *Gene therapy* **1998,** *5* (4), 542-51; (b) Balci, B.; Dincer, P., Efficient transfection of mouse-derived C2C12 myoblasts using a matrigel basement membrane matrix. *Biotechnology journal* **2009,** *4* (7), 1042-5.

5. (a) Cormier-Regard, S.; Nguyen, S. V.; Claycomb, W. C., Adrenomedullin gene expression is developmentally regulated and induced by hypoxia in rat ventricular cardiac myocytes. *The Journal of biological chemistry* **1998,** *273* (28), 17787-92; (b) Djurovic, S.; Iversen, N.; Jeansson, S.; Hoover, F.; Christensen, G., Comparison of nonviral transfection and adeno-associated viral transduction on cardiomyocytes. *Molecular biotechnology* **2004,** *28* (1), 21-32; (c) Louch, W. E.; Sheehan, K. A.; Wolska, B. M., Methods in cardiomyocyte isolation, culture, and gene transfer. *Journal of molecular and cellular cardiology* **2011,** *51* (3), 288-98.

6. Gizak, A.; Maciaszczyk-Dziubinska, E.; Jurowicz, M.; Rakus, D., Muscle FBPase is targeted to nucleus by its 203KKKGK207 sequence. *Proteins* **2009,** *77* (2), 262-7.

7. (a) Wang, Y.; Deng, X.; Mancarella, S.; Hendron, E.; Eguchi, S.; Soboloff, J.; Tang, X. D.; Gill, D. L., The calcium store sensor, STIM1, reciprocally controls Orai and CaV1.2 channels. *Science* **2010,** *330* (6000), 105-9; (b) Liu, N.; Liu, Y.; Yang, Y.; Liu, X., Linker flexibility of IVS3-S4 loops modulates voltage-dependent activation of L-type Ca(2+) channels. *Channels* **2017,** *11* (1), 34-45.

Supplemental Figures

(a)

(b)

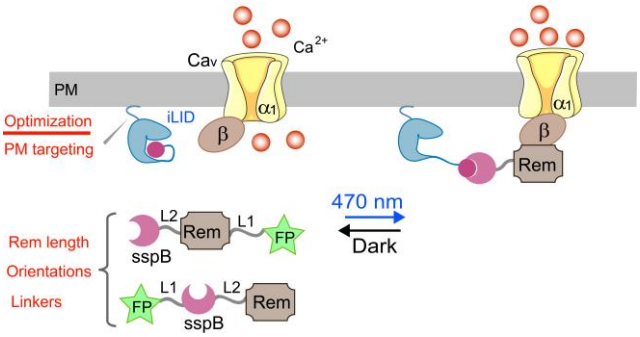

Venus-iLID-CAAX + mCh-L1-sspB-L2-Rem$_{1-266}$	Cytosol-to-PM translocation		KCl induced Ca^{2+} influx	
	Dark	Light	Dark*	Light
L1 = GS; L2 = EF	–	–	+++	+++
L1 = GSGGS; L2= EFGSGGGGSGS	–	+ +	+++	++
Venus-iLID-CAAX + mCh-L1-Rem$_{1-266}$-L2-sspB				
L1 = GSGGS; L2= EFGSGGGGSGS	–	+ + +	+++	+
Lyn11-iLID-GFP + mCh-L1-Rem$_{1-266}$-L2-sspB				
L1 = GSGGS; L2= EFGSGGGGSGS	–	+ +	+++	++

Figure S1: Design and characterization of engineered optoRGK constructs.

(a) Domain architecture of the human Rem. Rem$_{1-266}$ lacking the C-terminal PM targeting sequence mainly locates in the cytosol and fails to suppress $Ca_V1.2$ channels. Rem$_{1-266}$ can recover its inhibitory function on Ca_V channels by introducing other proteins' PM targeting sequences. Herein, we engineered Rem by incorporating the optical dimerizer based on iLID (LOV2-ssrA) and sspB to photo-control its cytosol-to-PM translocation, thereby remotely modulating Ca_V channels.

(b) (*Left*) Schematic illustrating the light-dependent translocation of Rem$_{1-266}$ from cytosol to plasma membrane by fusing sspB with Rem, while iLID tethered to PM. (*Right*) Summary of optogenetic performance of designed chimeric constructs. To obtain an engineered Rem showing good PM translocation, we optimized the linkers and the relative positioning of different components. The PM translocation efficiency of engineered Rems is gauged by the ratio of $F_{PM}/(F_{Cytosol} + F_{PM})$ in the dark and light conditions. F_{PM} represents the fluorescent intensity of PM-bound Rem, while $F_{Cytosol}$ means the fluorescent intensity of Rem in the cytosol. The values were defined as follows: −, < 0.3 PM-resident components; +, 0.3 ~ 0.6; ++, 0.6 ~ 0.8; +++, 0.8 ~ 1. For KCl triggered Ca^{2+} influxes, the dynamic range, reported by the averaged changes in the fluorescence intensities ($\Delta F/F_0$) of the Ca^{2+} sensor jRCaMPs, was categorized as follows: "−", < 1.0; "+", 1.0 ~ 2.0; "++", 2.0 ~ 3.0; "+++", > 3.0. The combination of iLID-CAAX and mCh-L1-Rem$_{1-266}$-L2-sspB (L1 = GSGGS; L2= EFGSGGGGSGS) showed the best performance and was named as optoRGK.

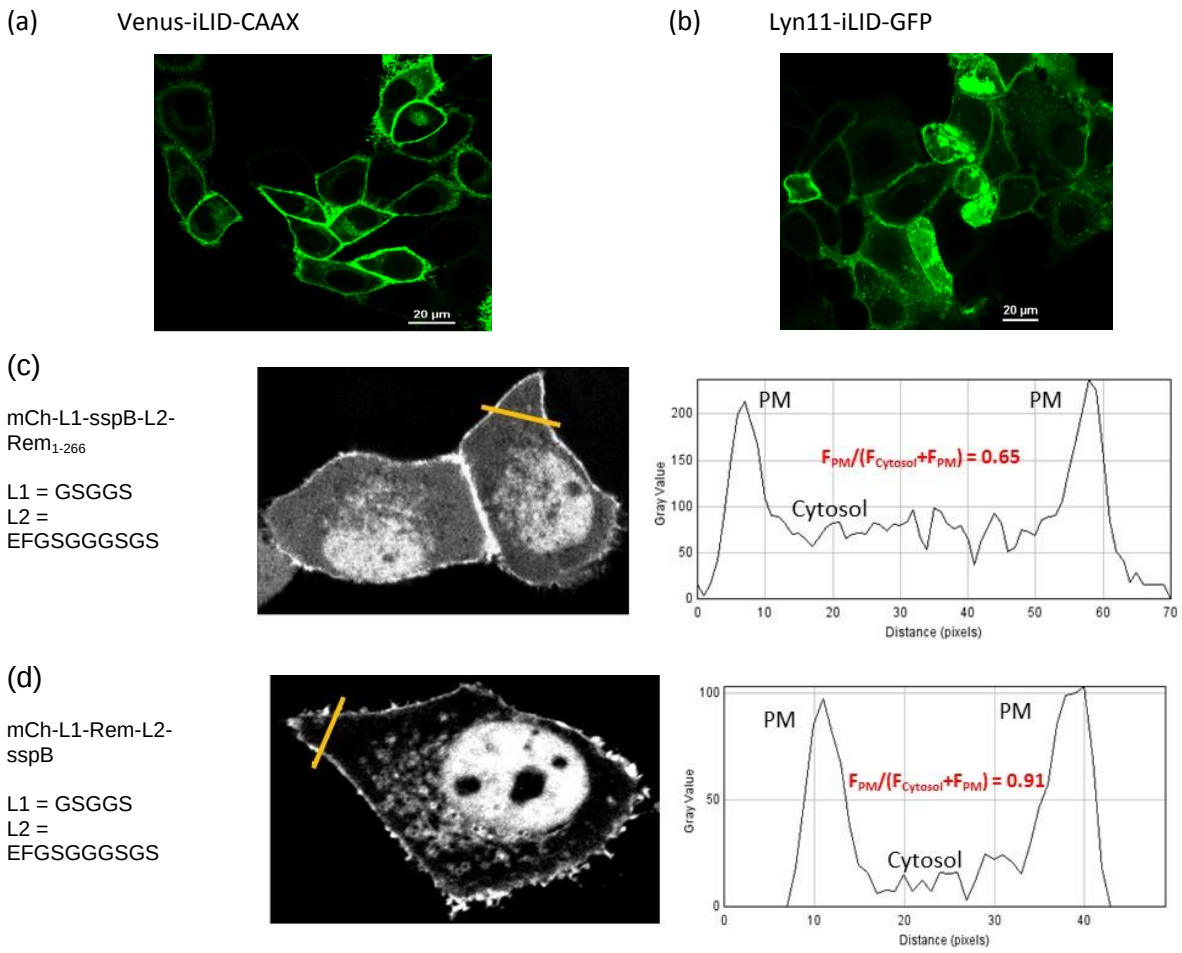

Figure S2: **Comparison of PM-targeting motifs used to anchor iLID to PM, which could subsequently recruit mCherry-tagged sspB-Rem variants toward PM.**

(a-b) Confocal images showing the localization of Venus-iLID-CAAX (a) or Lyn11-iLID-GFP (b) in HeLa cells. Venus-iLID-CAAX showed better PM decoration with minimized cytosolic aggregation when comparing to Lyn11-iLID-GFP. We therefore used the CAAX motif for PM recruitment.

(c-d) Representative confocal images of mCh-L1-sspB-L2-Rem_{1-266} (a) and mCh-L1-Rem-L2-sspB (b) after blue light exposure with coexpression of Venus-iLID-CAAX (Left). Along the yellow lines of confocal images of transfected cells, the corresponding fluorescence intensities were plotted (right). The resulting $F_{PM}/(F_{Cytosol} + F_{PM})$ ratio was shown in red.

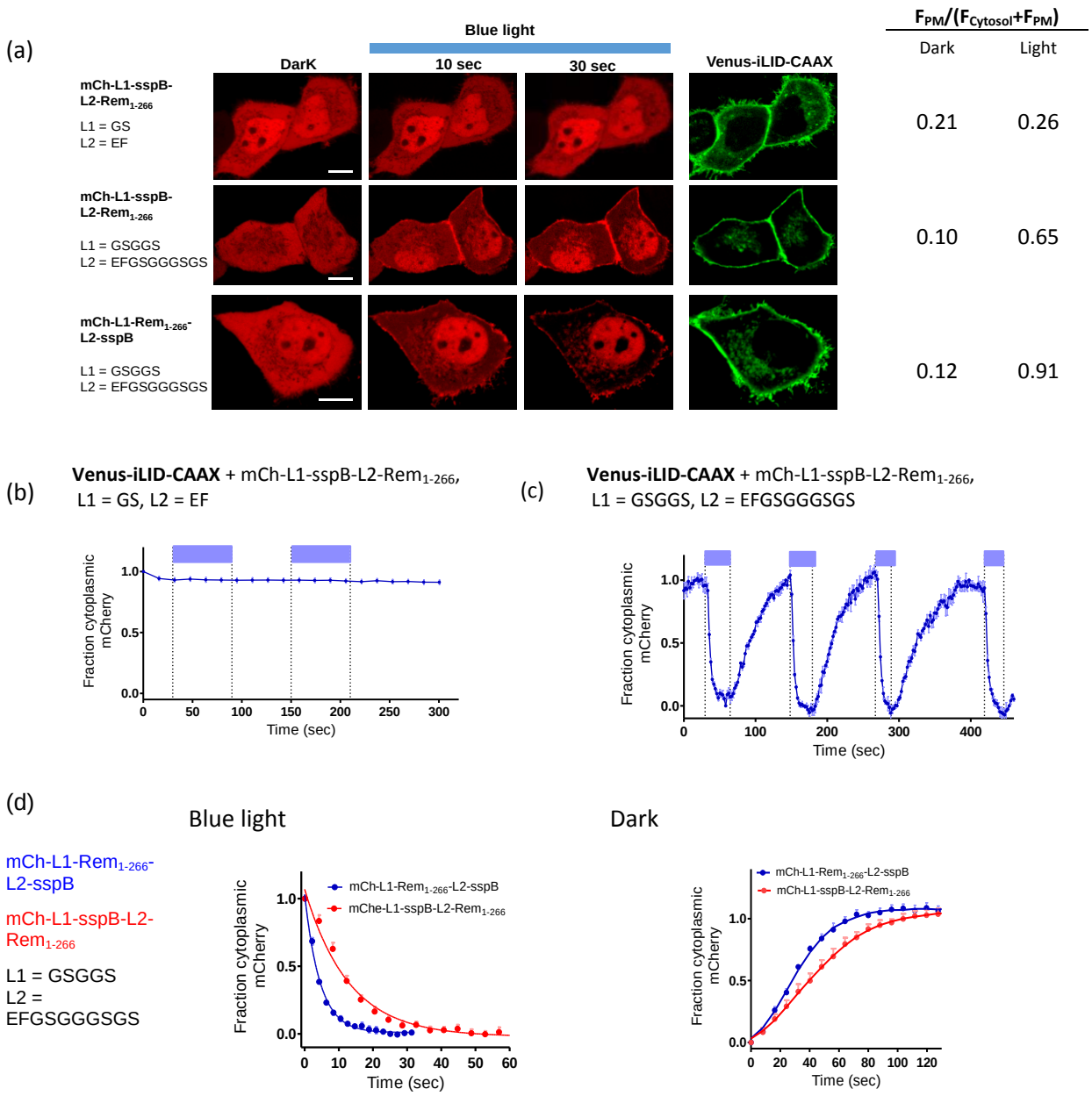

Figure S3: **Optimization of light-inducible cytosol-to-PM translocation for engineered optoRGK constructs.**

(a) (Left) Light-inducible translocation of the indicated chimeric constructs (sspB fused with mCh-Rem$_{1-266}$) from the cytosol to the plasma membrane in HeLa cells co-expressing Venus-iLID-CAAX. *Upper* panel, mCh-L1-sspB-L2-Rem$_{1-266}$, L1 = GS, L2 = EF. This version showed no translocation after blue light illumination; *Middle* panel, mCh-L1-sspB-L2-Rem$_{1-266}$, L1 = GSGGS, L2 = EFGSGGGSGS; *Bottom* panel, mCh-L1-Rem$_{1-266}$-L2-sspB, L1 = GSGGS, L2 = EFGSGGGSGS. (Right) The translocation efficiency (indicated by the ratio: $F_{PM}/(F_{Cytosol} + F_{PM})$) of mCh tagged Rems in the dark and lit conditions. More than 20 cells for each group were selected from three independent experiments.

(b-c) Quantification of mCherry signals in cells expressing the indicated constructs over repeated light-dark cycles (n > 20 cells) from three independent experiments. An external blue LED was used to photoactivate the transfected cells at 470 nm (40 µW/mm^2; blue bar). Scale bar, 10 µm. Error bars denote s.e.m..

(d) Comparison of the activation (left, blue light illumination) and inactivation kinetics (right, dark) of PM-to-Cytosol translocation between mCh-Rem_{1-266}-sspB (blue, corresponding to Fig 1b) and mCh-sspB-Rem_{1-266} (red, blue, corresponding to Fig S3c) when coexpressed with Venus-iLID-CAAX in HeLa cells. Both mCh-Rem_{1-266}-sspB ($t_{1/2,\ on}$ = 3.2 ± 1.0 sec; $t_{1/2,\ off}$ = 23.0 ± 2.4 sec) and mCherry-sspB-Rem_{1-266} ($t_{1/2,\ on}$ = 8.9 ± 1.2 sec; $t_{1/2,\ off}$ = 39.6 ± 3.2 sec) underwent rapid cytosol-to-PM translocation in response to blue light illumination, but the latter construct showed a relatively slower kinetics.

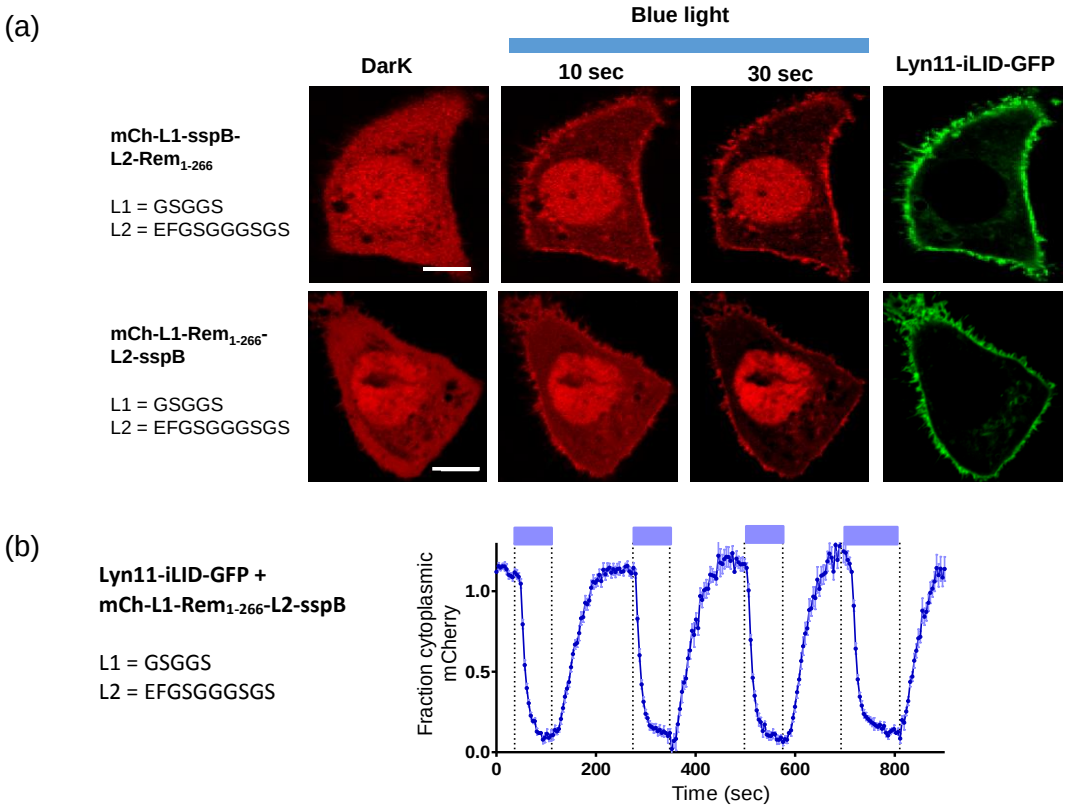

Figure S4: **Light-inducible translocation of mCh-tagged Rem_{1-266} chimeras from cytosol to plasma membrane in HeLa cells expressing Lyn11-iLID-GFP**.

(a) Confocal images showing blue light-dependent PM translocation of mCh-L1-sspB-L2-Rem_{1-266} (*upper* panel) or mCh-L1-Rem_{1-266}-L2-sspB (*lower* panel) in HeLa cells co-transfected with PM-anchored Lyn11-iLID-GFP. L1 = GSGGS and L2 = EFGSGGGSGS. Scale bar, 10 µm.

(b) Quantification of cytosolic mCherry signals over three repeated light-dark cycles. Blue bar, light illumination at 470 nm with a power density of 40 µW/mm^2. n = 15 cells from three independent experiments. Error bars denote s.e.m..

(a)

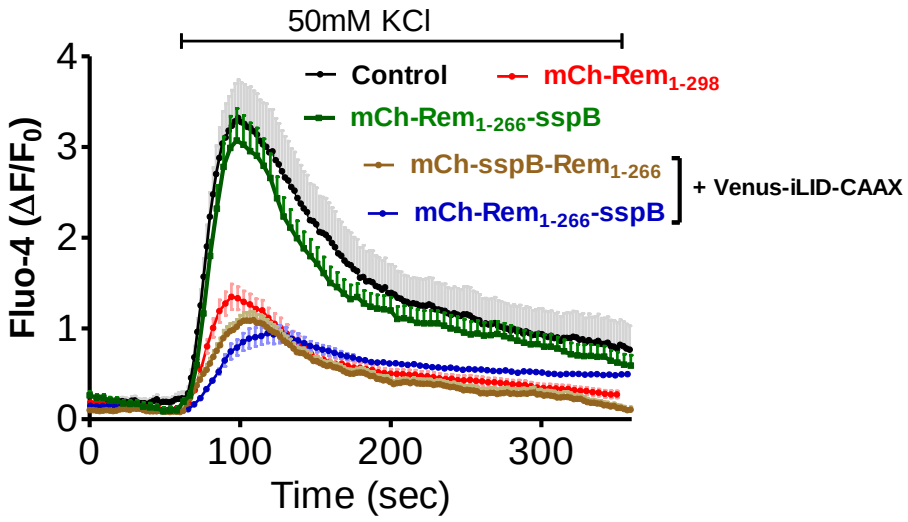

(b)

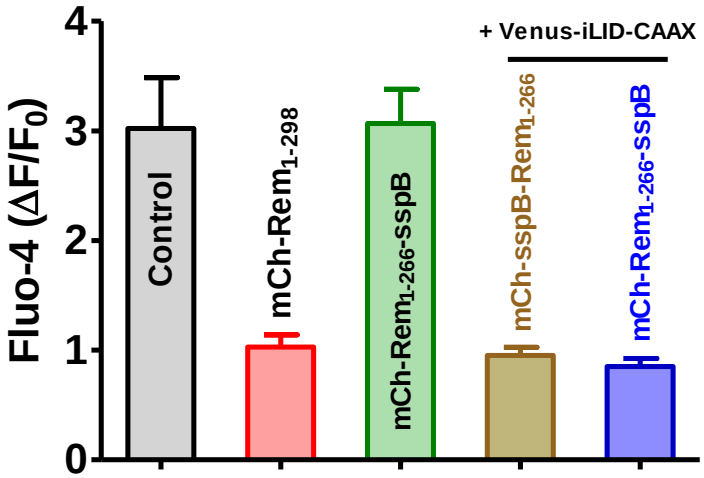

Figure S5: **Optogenetically engineered Rem caused photoactivatable inhibition of Ca^{2+} entry in C2C12 cells**.

(a) 50 mM KCl induced Ca^{2+} transients (Fluo-4 intensity as readout) in C2C12 cells expressing the indicated constructs, including mCh-Rem_{1-298} (positive control; red), the single construct of mCh-L1-Rem_{1-266}-L2-sspB (negative control; green), mCh-L1-Rem_{1-266}-L2-sspB (blue) or mCh-L1-sspB-L2- Rem_{1-266} (brown) with co-expression of Venus-iLID-CAAX. L1 = GSGGS and L2 = EFGSGGGSGS. The Ca^{2+} influx in untransfected cells from the group of optoRGK (mCh-L1-Rem_{1-266}-L2-sspB /Venus-iLID-CAAX) was showed as another native control (black). Fluo-4 signals were acquired by excitation with a 488-nm laser, which would simultaneously activate the optoRGK system to inhibit Ca_V channels. (b) Bar graphs showing the statistical results of peak Fluo-4 intensities in C2C12 cells expressing the indicated constructs. All data were presented as mean ± s.e.m. n = 22 cells from three independent experiments.

(a)

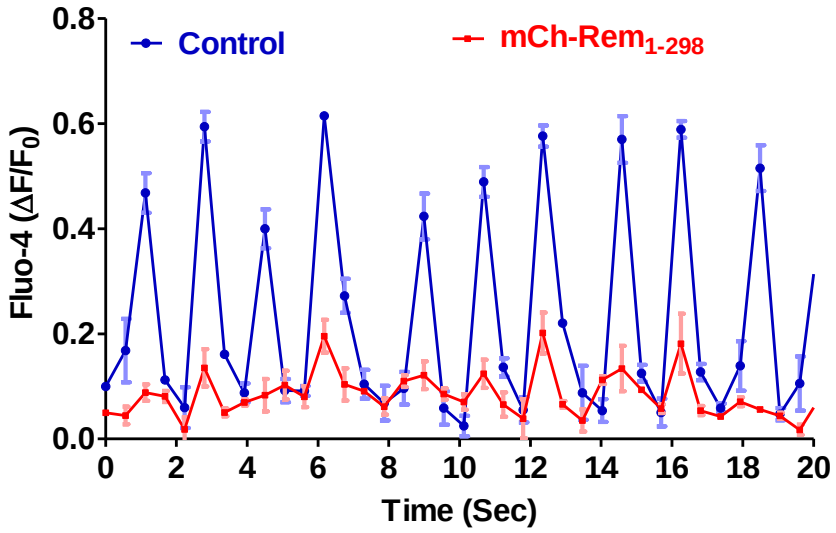

(b)

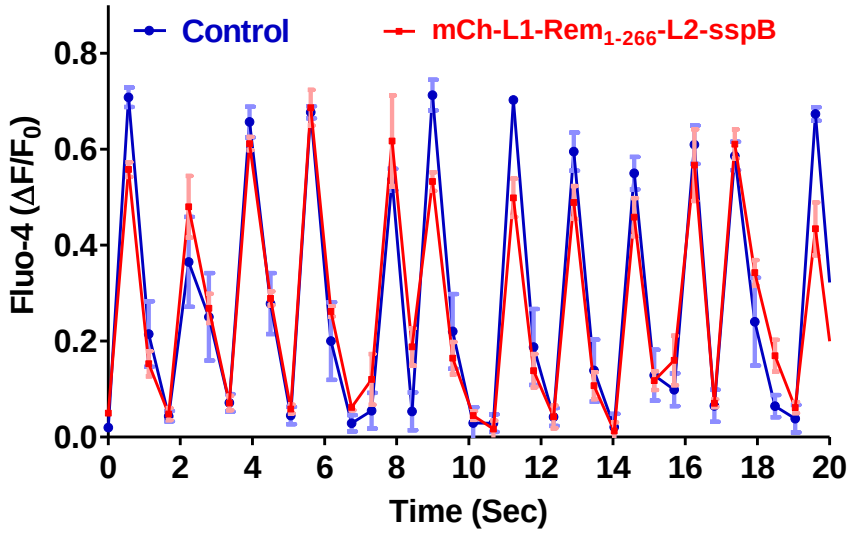

Figure S6: **Spontaneous Ca^{2+} transients recorded from Flou-4 loaded HL-1 cardiomyocytes.**

(a) Representative Fluo-4 intensity recordings from untransfected HL-1 cells (blue) or HL-1 cells transfected with mCh-Rem_{1-298} (red). mCh-Rem_{1-298} (full length) showed a potent inhibition of the spontaneous Ca^{2+} oscillation in HL-1 cells. Error bars denote s.e.m. n = 3 cells from neighbouring region.

(b) Representative recordings from untransfected HL-1 cells (blue) or cells expressing mCh-L1-Rem_{1-266}-L2-sspB (red) (L1 = GSGGS and L2 = EFGSGGGSGS). The truncation of the C-terminal PM-targeting sequence (aa 267-298) rendered Rem_{1-266} unable to suppress Ca^{2+} oscillation in HL-1 cells. Error bars denote s.e.m. n = 4 cells from neighbouring region.

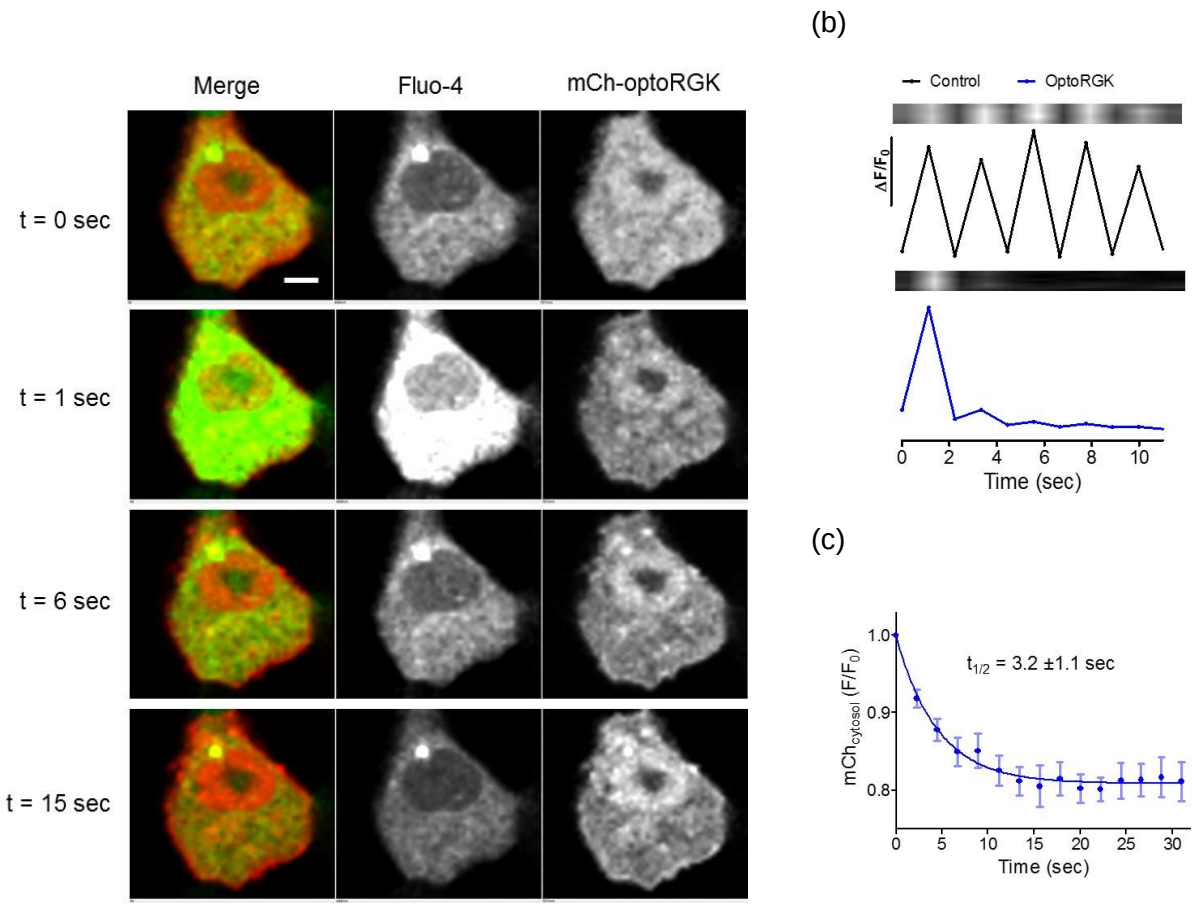

Figure S7: Blue light induced inhibition of spontaneous Ca^{2+} transients in HL-1 cardiomyocytes.

(a) Representative confocal images of Fluo-4 loaded HL-1 cells expressing optoRGK (mCh-L1-Rem1$_{1-266}$-L2-sspB-P2A-iLID-CAAX, L1 = GSGGS and L2 = EFGSGGGSGS) under blue light. Both 488-nm and 561-nm channels were used to excite Fluo-4 and mCherry signals, respectively. Within the first 2 sec, we observed one Ca^{2+} transient and optoRGK largely remained in the cytosol. Thereafter, we noticed that a portion of mCh-optoRGK translocated to PM (red), accompanied with a decrease in the intracellular Ca^{2+} signals reported by Fluo-4 (green; at time point 30 sec). Scale bar, 5 μm.

(b) Spontaneous Ca^{2+} transients acquired in untransfected HL-1 cells (upper, black) or cells expressing optoRGK (bottom, blue) under blue light. Kymograph of Fluo-4 was shown above the corresponding curves.

(c) The photo-activated PM translocation of mCh-Rem$_{1-266}$-sspB reflected by the changes in the cytosolic intensities of mCherry fluorescence. The half-life of this photoactivation process was determined to be 3.2 ± 1.1 sec. n = 12 cells from three independent experiments. Error bars denote s.e.m..

Supplemental Movies

Movie S1. Visualization of reversible recruitment of mCh-optoRGK to the plasma membrane in response to blue light (470 nm, 40 μW/mm^2) stimulation in HeLa cells.

Movie S2. Spontaneous rhythmic oscillations of cytosolic Ca^{2+} in HL-1 cells measured by the green fluorescent calcium indicator, Fluo-4. (Top) Ca^{2+} transients were measured in untransfected HL-1 cells using Fluo-4 dye; (Bottom) The time course of Fluo-4 signals in multiple selected regions in HL-1 cells.

Movie S3 Rhythmic Ca^{2+} oscillations in HL-1 cells were inhibited with overexpression of the full length Rem_{1-298}.

(Top) Time series of confocal images with the montage of multiple channels showing Ca^{2+} transients in untransfected and transfected (mCh-Rem_{1-298}) HL-1 cells. (Bottom) Comparison of Fluo-4 signals between untransfected (region 2, green curve) and transfected (mCh-Rem_{1-298}, region 1, red curve) HL-1 cells.

Movie S4 Rem with C-terminal truncation (Rem_{1-266}) showed no overt inhibition on spontaneous Ca^{2+} oscillations in HL-1 cells. (Top) Time series of confocal images with the montage of multiple channels showing Ca^{2+} transients in transfected (mCh-L1-Rem_{1-266}-L2-sspB, L1 = GSGGS and L2 = EFGSGGGSGS) HL-1 cells. (Bottom) Fluo-4 signals in multiple selected regions in HL-1 cells expressing of Rem_{1-266}.

Movie S5 OptoRGK showed light-inducible suppression on cytosolic Ca^{2+} oscillations in HL-1 cells.

(Top) Confocal images of Fluo-4 (green) loaded HL-1 cells that were transfected with mCh-optoRGK (red). Following blue light exposure, a portion of mCh-optoRGK migrated from the cytosol toward the PM.

(Middle) Time series of confocal images showing Ca^{2+} transients in untransfected (region 2 and 3) and transfected (mCh-optoRGK, region 2) HL-1 cells.

(Bottom) Comparison of Fluo-4 signals in untransfected (region 2 and 3; green curve and blue curve) and transfected (region 1, red curve) cells. 488-nm channel for exciting Fluo-4 emission was also used as the visible light source to activate optoRGK (photo-activation window: 400-500 nm).